EAST EUROPEAN JOURNAL OF PHYSICS
East Eur. J. Phys. Vol.4 No.3 (2017) 54-62 DOI:10.26565/2312-4334-2017-3-08

PACS: 87.14.Cc, 87.16.Dg

MOLECULAR DYNAMICS STUDY OF CYTOCHROME *C* – LIPID COMPLEXES

V. Trusova, G. Gorbenko, U. Tarabara, K. Vus, O. Ryzhova
Department of Nuclear and Medical Physics, V.N. Karazin Kharkiv National University
4 Svobody Sq., Kharkiv, 61022, Ukraine
e-mail: valerija.trusova@karazin.ua
Received August 1, 2017

The interactions between a mitochondrial hemoprotein cytochrome *c* (cyt *c*) and the model lipid membranes composed of zwitterionic lipid phosphatidylcholine (PC) and anionic lipids phosphatidylglycerol (PG), phosphatidylserine (PS) or cardiolipin (CL) were studied using the method of molecular dynamics. It was found that cyt *c* structure remains virtually unchanged in the protein complexes with PC/PG or PC/PS bilayers. In turn, protein binding to PC/CL bilayer is followed by the rise in cyt *c* radius of gyration and root-mean-square fluctuations. The magnitude of these changes was demonstrated to increase with the anionic lipid content. The revealed effect was interpreted in terms of the partial unfolding of polypeptide chain in the region Ala15-Leu32, widening of the heme crevice and enhancement of the conformational fluctuations in the region Pro76-Asp93 upon increasing the CL molar fraction from 5 to 25%. The results obtained seem to be of utmost importance in the context of amyloidogenic propensity of cyt *c*.
KEYWORDS: cytochrome c; protein-lipid interactions; amyloid, molecular dynamics

МОЛЕКУЛЯРНО-ДИНАМІЧНЕ ДОСЛІДЖЕННЯ КОМПЛЕКСІВ ЦИТОХРОМУ *С* З ЛІПІДАМИ
В. Трусова, Г. Горбенко, У. Тарабара, Е. Вус, О. Рижова
Кафедра ядерної та медичної фізики, Харківський національний університет імені В.Н. Каразіна
пл. Свободи 4, Харків, 61022, Україна
Методом молекулярної динаміки досліджено взаємодію мітохондріального гемопротеїну цитохрому *с* з модельними мембранами, що складались із цвіттеріонного ліпіду фосфатидилхоліну (ФХ) та аніонних ліпідів фосфатидилгліцерину (ФГ), фосфатидилсерину (ФС) чи кардіоліпіну (КЛ). Показано, що структура цитохрому *с* залишається практично незмінною у комплексах білка з ФХ/ФГ чи ФХ/ФС бішарами. У свою чергу, зв'язування білка із ФХ/КЛ бішарами супроводжується збільшенням радіусу інерції та середньоквадратичних флуктуацій цитохрому *с*. Продемонстровано, що величина цих змін зростає із вмістом аніонного ліпіду. Винайдені ефекти були інтерпретовані у рамках часткового розгортання поліпептидного ланцюга в області Ala15-Leu32, розширення гемового карману та посилення конформаційних флуктуацій на ділянці Pro76-Asp93 при зростанні молярної частки КЛ від 5 до 25%. Отримані результати важливі у контексті амілоїдогенної здатності цитохрому *с*.
КЛЮЧОВІ СЛОВА: цитохром *с*, білок-ліпідні взаємодії, амілоїд, молекулярна динаміка

МОЛЕКУЛЯРНО-ДИНАМИЧЕСКОЕ ИССЛЕДОВАНИЕ КОМПЛЕКСОВ ЦИТОХРОМА *С* С ЛИПИДАМИ
В. Трусова, Г. Горбенко, У. Тарабара, Е. Вус, О. Рыжова
Кафедра ядерной и медицинской физики, Харьковский национальный университет имени В.Н. Каразина
пл. Свободы 4, Харьков, 61022, Украина
Методом молекулярной динамики исследовано взаимодействие митохондриального гемопротеина цитохрома *с* с модельными мембранами, состоящими из цвиттерионного липида фосфатидилхолина (ФХ) и анионных липидов фосфатидилглицерина (ФГ), фосфатидилсерина (ФС) или кардиолипина (КЛ). Показано, что структура цитохрома *с* остается практически неизменной в комплексах белка с ФХ/ФГ или ФХ/ФС бислоями. В свою очередь, связывание белка с ФХ/КЛ бислоями сопровождается увеличением радиуса инерции и величины среднеквадратичных флуктуаций цитохрома *с*. Продемонстрировано, что величина этих изменений возрастает с содержанием анионного липида. Выявленные эффекты были интерпретированы в рамках частичного разворачивания полипептидной цепи в области Ala15-Leu32, расширение гемового кармана и усиление конформационных флуктуаций на участке Pro76-Asp93 при возрастании молярной доли КЛ от 5 до 25%. Полученные данные важны в контексте амилоидогенной способности цитохрома *с*.
КЛЮЧЕВЫЕ СЛОВА: цитохром *с*, белок-липидные взаимодействия, амилоид, молекулярная динамика

One-dimensional crystallization of the proteins and peptides into highly ordered fibrillar structures, termed amyloids, is a key factor in etiology of a number of disorders, including Alzheimer's, Parkinson's, Huntingtons diseases, type II diabetes, rheumatoid arthritis, spongiform encephalophaties, etc [1]. Amyloid fibrils are distinguished by a core cross-β-sheet structure in which β-strands run perpendicularly to the long axis of the fibril, while β-sheets propagate in its direction [2]. Amyloid assembly is a hierarchical process that is currently regarded as alternative folding [3], since both the intrachain and interchain contacts are governed by the common forces, *viz.* hydrophobic effect, hydrogen-bonding, charge attraction and van der Waals interactions [4]. Protein oligomerization followed by amyloid formation is commonly initiated by the transition of polypeptide chain into unstable aggregation-competent conformation [5]. Since the compactness of native state is compromised by the loss of configurational entropy during polypeptide folding and repulsive electrostatic interactions, the native protein structure is only marginally stable and any variation in physicochemical properties of polypeptide environment may prove critical for protein transition from monomeric to aggregated state [6]. In vitro, fibrillization-favoring conditions are created by lowering pH, elevating temperature,

adding organic solvents or denaturants, etc., while in vivo, aggregation-competent conformation may arise from mutations, oxidative or heat stress, or destabilization of the protein structure upon its adsorption at interfaces. It is the presence of large amount of interface, formed by cellular membranes, that determines the principal difference between in vitro and in vivo amyloid growth. Lipid bilayer, a basic structural element of biological membranes, may act as an effective catalyst of fibrillogenesis, providing an environment where protein molecules accumulate and adopt conformation and orientation promoting their assembly into protofibrillar and fibrillar structures. The problem of membrane-mediated fibrillogenesis has been approached in a number of works, demonstrating the complexity and multiplicity of factors which may control fibrillogenesis in membrane systems [7-9]. It has been hypothesized that anionic phospholipids represent the main membrane component responsible for the enhancement of fibril formation, as shown, particularly, for α-synuclein [10], Aβ peptide [7], amylin [11], tau [12], lysozyme, transthyretin, cytochrome c, insulin, myoglobin [13]. An increasing number of studies provides support to the idea that lipid bilayer can lower the activation energy barrier for protein unfolding [14]. Partial unfolding in a membrane environment has been reported, for instance, for phospholipase A2, bacterial toxins, acetylcholinesterase, pheromone-binding protein, recombinant human prion protein, etc [15]. The role of lipids as a structure-forming environment is not restricted to electrostatic phenomena (lowered interfacial pH or neutralization of the protein surface charge by anionic headgroups), other bilayer characteristics may have an impact on the protein structure as well. It is becoming increasingly apparent that development of effective anti-amyloid strategies is impossible without elucidating the mechanisms by which lipids promote transition of the protein molecule into aggregation-competent conformation. One of the powerful modern tools to address this problem is the method of molecular dynamics (MD). This method is highly suitable for uncovering the atomistic level details of polypeptide conformational changes in solution and in a membrane environment [16,17], protein folding and misfolding [18,19], the assembly of prefibrillar and fibrillar aggregates [20], etc.

The aim of the present study involves the use of MD simulation to gain insight into the role of acidic phospholipids in the occurrence of potentially amyloidogenic conformations of cytochrome *c* (cyt *c*), a basic protein playing an essential role in the electron transfer in the respiratory chain of the inner mitochondrial membrane and programmed cell death, apoptosis [21,22]. It has been demonstrated that cyt *c* is capable of forming amyloid fibrils in vitro, although the physiological significance of this property is not clear [23-25]. Nevertheless, α-synuclein and cyt *c* have been found to be colocalized in Lewy bodies of patients with Parkinson's disease [26]. It has been hypothesized that there exists yet unknown link between apoptosis and neurodegeneration [23,26]. Therefore, examining the conformational dynamics of cyt *c* in various environments is of great importance for understanding the determinants and physiological role of amyloidogenic propensity of this protein.

MATERIALS AND METHODS

Molecular dynamics simulations were performed with GROMACS software (version 5.1) using the CHARMM36 force field [B33]. The calculations were done at a temperature of 310 K and a pressure of 1 bar. The crystal structure of horse heart cytochrome c (PDB ID: 1HRC) was used as a starting structure for simulations. The orientation of the protein with respect to the lipid/water interface was predicted using the PPM server [B34]. The input files for MD calculations were prepared using the web-based graphical interface CHARMM-GUI [B35]. The lipid bilayers were built from phosphatidylcholine (PC) and varying proportions of one of the anionic phospholipids, cardiolipin (CL, 5, 11 and 25 mol%), phosphatidylglycerol (PG, 10, 20 and 40 mol %) or phosphatidylserine (PS, 10, 20 and 40 mol %). The protein was solvated in the rectangular box with a minimum distance of 10 Å to the edges of the box. The TIP3P water model was used. To obtain a neutral total charge of the system a necessary number of counterions was added. For correct treatment of long-range electrostatic interactions, Particle Mesh Ewald algorithm was employed [B36]. The minimization and equilibration of the system were performed during 100 ps and 1 ns, respectively. The time step for MD simulations was 2 fs. The trajectories and coordinates were saved every 2 ps for further analysis. The whole time interval for MD calculations was 100 ns. The analysis tools included in GROMACS were used to calculate the root-mean-square deviations (RMSD), root-mean-square fluctuations (RMSF) and radius of gyratio (Rg). The evolution of the secondary structure was followed using the VMD program. The contact maps were generated with the CMView software [B37]. The analysis of cyt *c* three-dimensional structure after the simulation was performed using PyMOL.

RESULTS AND DISCUSSION

Cytochrome *c* is a globular protein composed of 104 amino acid residues, with a high α-helical content and minimal β-sheet structure (Fig. 1). Under physiological conditions there exists an equilibrium between a soluble native and membrane-bound states of cyt *c* [32]. Biological functions of cyt *c* are mediated by its interaction with cardiolipin, an anionic mitochondrial phospholipid with unique physicochemical properties [33]. The cyt *c* molecule has been assumed to contain two types of binding sites for anionic phospholipids, accounting for electrostatic interactions between the residues Lys72, Lys73 and deprotonated phosphate group (A-site) and hydrogen bonding between Asn52 and protonated phosphate (C-site) [34].

Moreover, it has been supposed that upon cyt *c* – CL association through C-site one of four CL acyl chains extends outwards from the lipid bilayer into the protein hydrophobic channel close to Asn52, thereby ensuring the hydrophobic protein-lipid interactions [34]. The idea of extended lipid anchorage initially put forward by Rytomaa &

Kinnunen [35], was further developed by Kalanxni & Wallace who proposed that CL acyl chain accommodates in the nonpolar pocket situated in the vicinity of Met80 loop [36], while Sinibaldi et al. suggested the insertion of two fatty acid chains of CL into two different hydrophobic channels of cyt *c* surrounding Met80 and Asn52 [37]. Along with the diversity of the binding modes, another characteristic feature of cyt *c* – CL interaction is the heterogeneity of the protein conformational states [38-40]. CL was reported to produce the loosening of cyt *c* tertiary structure, destabilization of the secondary structure, loss of Met_{80} – iron ligation and opening of the heme crevice, eventually leading to the increase of the protein peroxidase activity [41-43].

Fig. 1. Crystal structure of the horse heart cytochrome c (PDB code 1HRC). Shown in red is the heme group

Recent studies provided evidence for the existence of multiple conformations of CL-bound cyt *c* differing in the degree of protein unfolding and undergoing the conformational exchange between the extended and compact subpopulations [38,44]. Remarkably, the alterations in the protein structure are strongly coupled with the molecular reorganization of CL-containing lipid bilayers [45-47]. Similar to other basic proteins, cyt *c* is capable of gathering the anionic phospholipids into microdomains, but cyt *c* – CL systems display particular behavior due to decreased energetic barrier for the formation of the inverted hexagonal (H_{II}) phase [46] and toroidal lipid pores [47]. All the above phenomena are conjectured to be of importance for both electron transfer and apoptotic functions of cyt *c* and may contribute to its amyloidogenic propensity. Notwithstanding considerable advances in molecular-level understanding of cyt *c* – CL interactions, the precise mechanisms of this process still remain to be fully elucidated. One of the unresolved questions is how specific features of CL distinguishing it from other anionic phospholipids operate in determining the structural and functional peculiarities of cyt *c* – CL complexes. To address this question, we performed the molecular dynamics simulation of cyt *c* complexes with PC/CL, PC/PS and PC/PG bilayers. Fig. 2 illustrates the disposition of cyt *c* molecule relative to the negatively charged lipid/water interface predicted by the PPM server. Remarkably, the protein orients in such a way that the residues Lys72 and Lys73 face the membrane surface and this orientation is generally retained during the MD simulation.

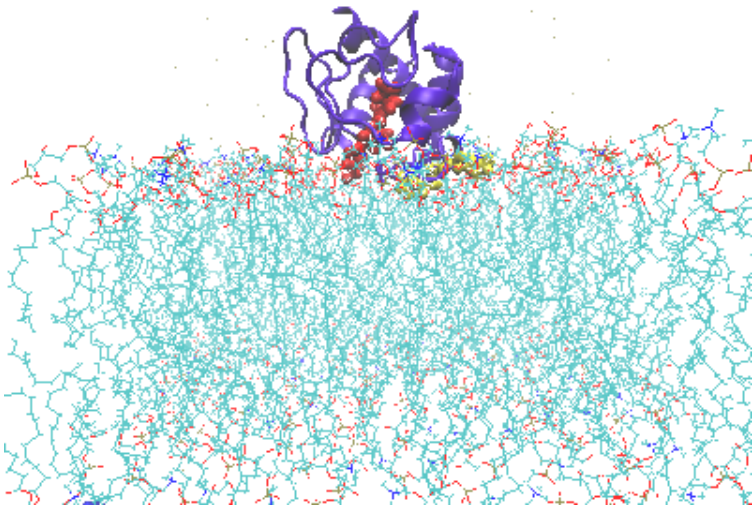

Fig. 2. Schematic illustration of the disposition of cyt *c* with respect to the lipid/water interface predicted by the PPM server. Shown in red is the heme group, while Lys72 and Lys73 are colored in yellow.

Figs. 3 and 4 represent the time course evolution of the two structural parameters of cyt *c* in the presence of lipid membranes – the radius of gyration (R_g) and root-mean-square fluctuations (RMSF) of C_α-atoms.

Notably, another parameter commonly used in the analysis of MD data, the backbone root-mean-square deviation (RMSD), did not show any significant difference between PC/CL, PC/PS and PC/PG systems suggesting that cyt *c* structure does not undergo considerable changes in a membrane environment within the examined time interval. At the same time, the radius of gyration was higher in CL-containing membranes, with the magnitude of this effect being increased with the molar content of CL (Fig. 3). Specifically, for the weakly charged lipid bilayers R_g was by ~7% higher in the presence of PC/CL membranes compared to PC/PG and PC/PS systems (Fig. 3A). The increase of the membrane charge resulted in ~11% (Fig. 3B) and ~14% (Fig. 3C) differences between CL- and PG/PS-containing bilayers. Similar tendencies were revealed while analyzing the root-mean-square fluctuations.

Concentrating on Fig. 4, it is clearly seen that: i) the residues Ala15-Leu32 experience much more pronounced

fluctuations compared to the other residues; ii) for CL-containing systems this effect is more conspicuous than for PC/PG or PC/PS bilayers; iii) the difference in RMSF values for the above protein region gradually increases with elevating the CL molar fraction, iv) the rise in CL content results in the enhancement of fluctuations in the region Pro76-Asp93. These findings led us to some preliminary conclusions: i) cyt *c* undergoes local conformational transitions in the region of Ala15-Leu32 and, to a lesser extent, in the region Pro76-Asp93; ii) these transitions are more specific for PC/CL lipid bilayers, as judged from the behavior of RMSF and R_g .

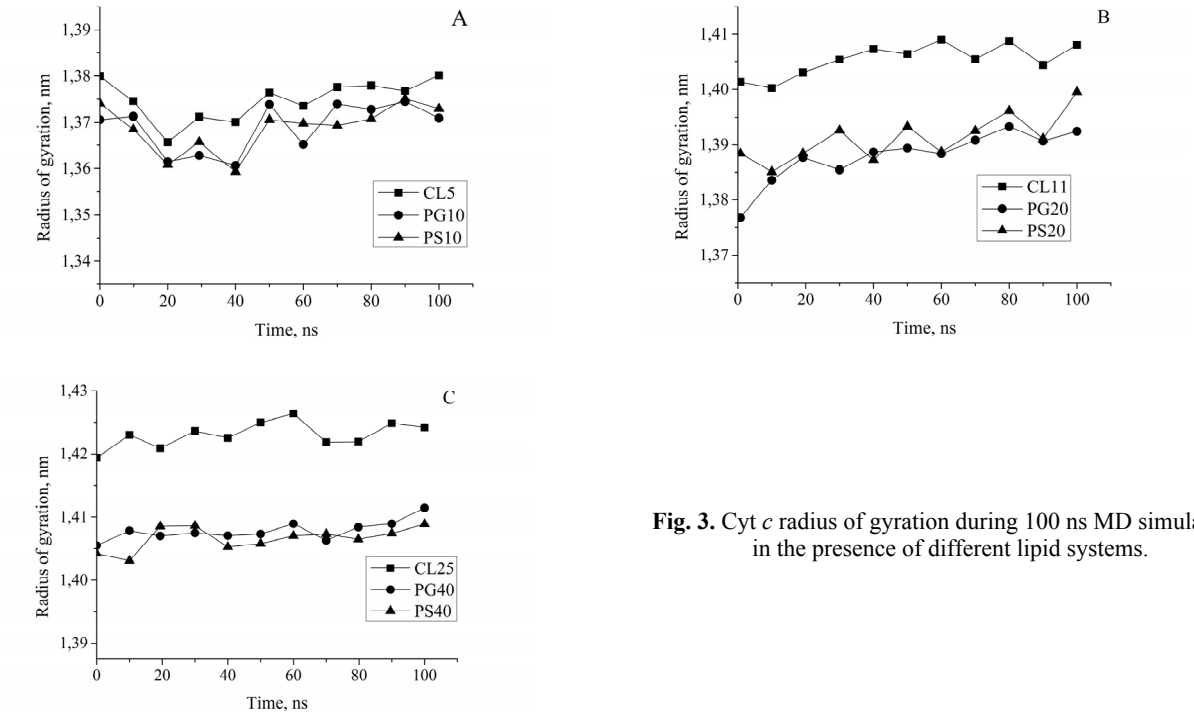

Fig. 3. Cyt *c* radius of gyration during 100 ns MD simulations in the presence of different lipid systems.

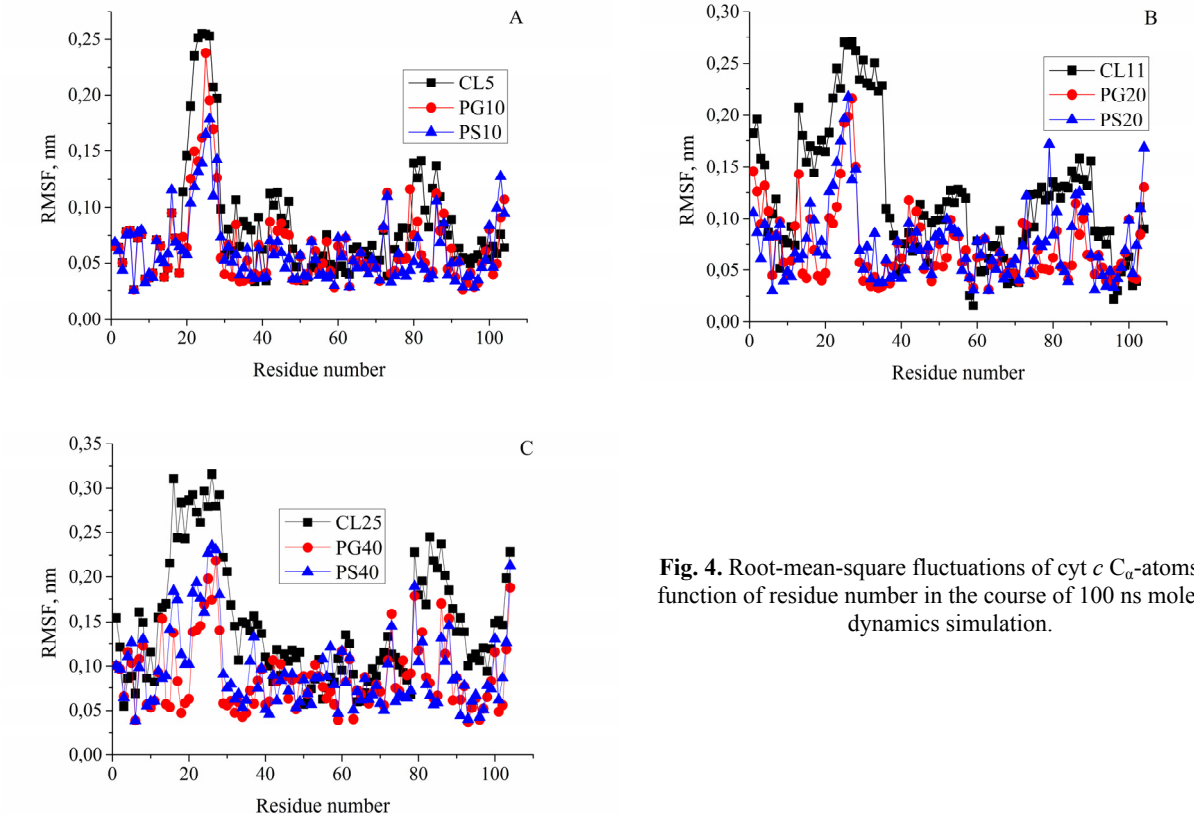

Fig. 4. Root-mean-square fluctuations of cyt *c* C_α-atoms as a function of residue number in the course of 100 ns molecular dynamics simulation.

In order to clarify what mechanism may be responsible for the aforesaid structural reorganization of polypeptide chain, we analyzed the time course of the changes in cyt *c* secondary structure. The representative plots are given in Fig. 5.

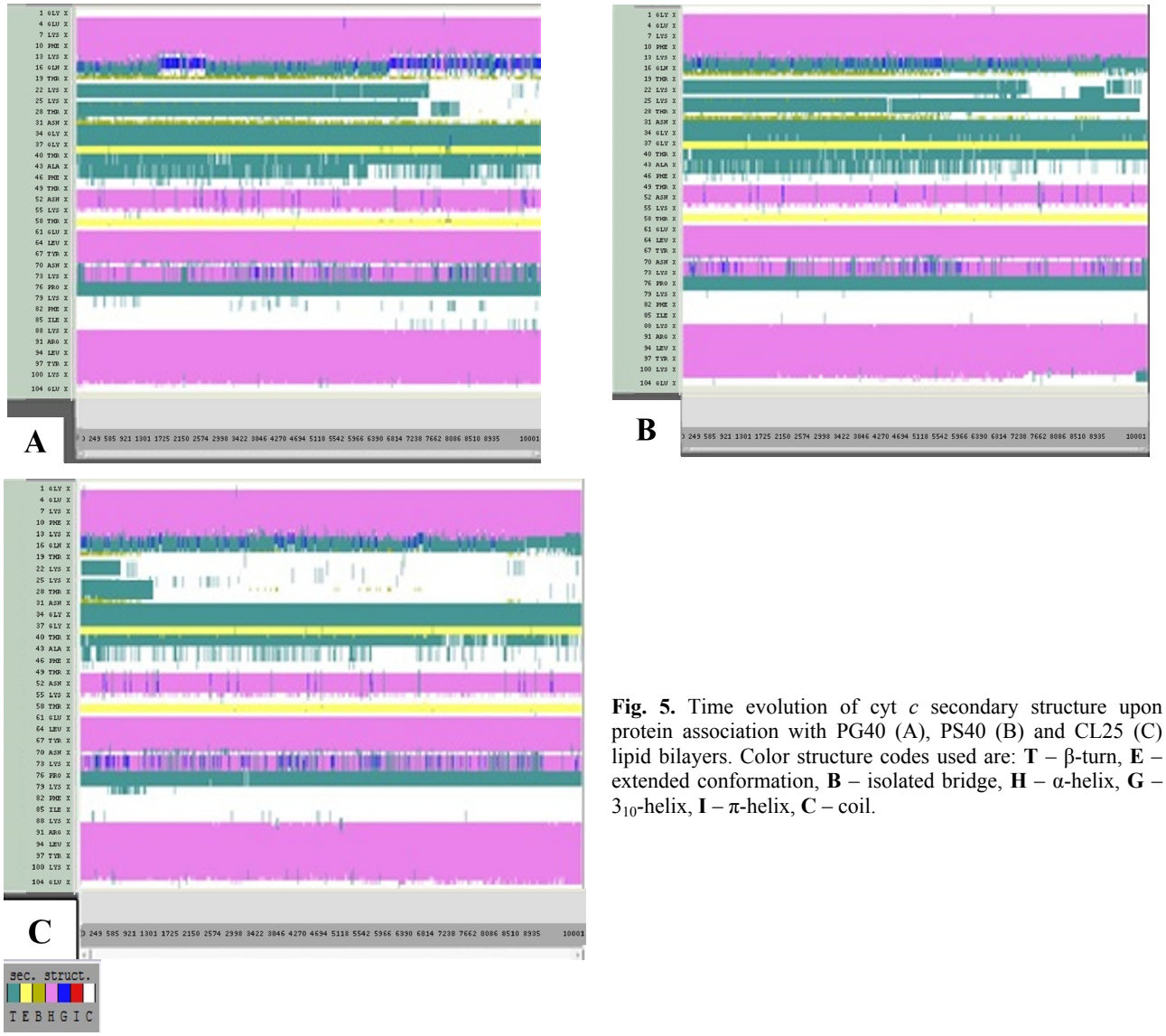

Fig. 5. Time evolution of cyt *c* secondary structure upon protein association with PG40 (A), PS40 (B) and CL25 (C) lipid bilayers. Color structure codes used are: **T** – β-turn, **E** – extended conformation, **B** – isolated bridge, **H** – α-helix, **G** – 3_{10}-helix, **I** – π-helix, **C** – coil.

It appeared that secondary structure of cyt *c* bound to PC/CL membranes differs from that observed in the presence of PC/PG or PC/PS lipid bilayers. Remarkably, the main difference involves the region Gln16-Asn31, the same fragment that was revealed by RMSF measurements. More specifically, in all cyt *c* – PC/PG(PS) systems the protein fragment Gln16-Asn31 adopts mostly turn conformation, while in cyt *c* – PC/CL complexes the unstructured (coiled) conformation of this region is predominant. Likewise, the content of coiled structures in the region Gln16-Asn31 increases with the molar fraction of CL, while in the presence of PC/PG(PS) membranes cyt *c* secondary structure was virtually independent of the proportion of anionic lipid. Furthermore, the comparison of timeline plots for cyt *c* free in solution (Fig. 5A) and those in the complexes with either PG- or PS-containing lipid bilayers (Figs. 5B and C) showed that the protein secondary structure undergoes slight alterations in these types of model membranes.

Notably, the peculiar features of CL-cyt *c* interactions have been revealed in the earlier studies [41,48,49]. More specifically, the affinity of cyt *c* for anionic phospholipids assessed by the surface plasmon resonance was found to decrease in the row: CL > PS > PC [49,50]. The solid-state ^{31}P NMR studies of cyt *c* interactions with CL, PS and PG bilayers showed that regardless the main driving force of all these interactions is electrostatic in nature, the structural alterations of the bound protein are lipid dependent [41,]. PS and CL were found to produce significant destabilization of cyt *c* structure, while in complexes with PG the protein retains a native-like conformation [41]. The resemblance between CL and PS in their effect on the structural state of cyt *c* was established in the early Raman [51,52] and ^{31}P NMR [50] studies. The two different conformational states of cyt *c* adsorbed on the negatively charged surfaces have been identified – the native-like state I and state II, with the opened heme crevice. The equilibrium between these two

states was supposed to be governed by the electrostatic interactions between lysine residues located around the heme crevice and the lipid phosphate groups. It was found that CL and PS promote the conformational equilibrium over the same temperature interval, while PG turned out to be less efficient in this respect, suggesting that cyt *c* conformation in complexes with PG is close to native [50]. A thorough recent work of Pandiscia & Schweitzer-Stenner provides evidence for an equilibrium between partially unfolded and native-like conformers of cyt *c* adsorbed on CL-containing bilayers, one of which forms electrostatic contacts with CL headgroups while the other one associates with lipids either via hydrogen bonding or hydrophobic interactions [40].

Overall, the MD data strongly suggest that lipid-induced conformational changes are specific for CL and involve the destabilization of the cyt *c* structure and partial unfolding of polypeptide chain in the region Gln16-Asn31, adjacent to the heme pocket. As indicated above, a great deal of experimental works provide evidence for partial unfolding of cyt *c* and opening of the heme crevice on the surface of CL-containing membranes [53-55]. One of the main mechanism underlying this phenomenon is assumed to involve the breakage of His26-Pro44 hydrogen bond [53,56]. It was shown that this bond plays a critical role in the stabilization of cyt *c* molecule [57], and its disruption triggers the destruction of Met80-heme ligation and opening of the heme crevice, the process resulting eventually in the loosening of the overall protein structure.

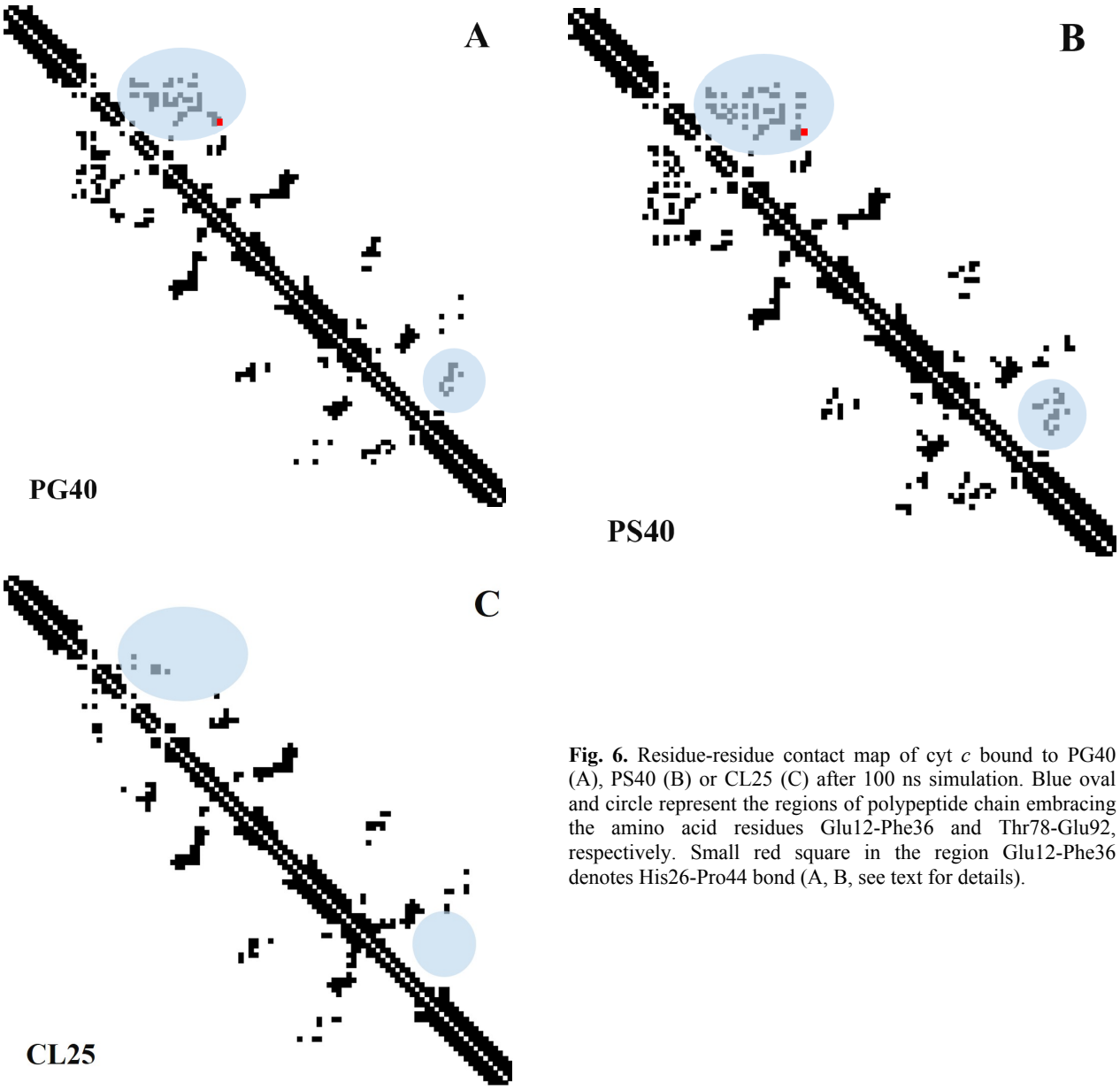

Fig. 6. Residue-residue contact map of cyt *c* bound to PG40 (A), PS40 (B) or CL25 (C) after 100 ns simulation. Blue oval and circle represent the regions of polypeptide chain embracing the amino acid residues Glu12-Phe36 and Thr78-Glu92, respectively. Small red square in the region Glu12-Phe36 denotes His26-Pro44 bond (A, B, see text for details).

Apparently, the described scenario manifests itself in the profiles of secondary structure evolution of cyt *c* recovered from the MD simulation of PC/CL lipid bilayers. Indeed, the comparison of cyt *c* inter-residue contact maps showed that His26-Pro44 bond is present in PC/PG or PC/PS (Figs. 6A and B) membranes, but disrupts when cyt *c*

binds to PC/CL bilayers (Fig. 6C). Furthermore, the contact maps are virtually identical for PC/PG and PC/PS systems, while cyt *c* complexation with PC/CL bilayers is accompanied by the reduction of the number of contacts, predominantly in the regions Glu12-Phe36 and Thr78-Glu92. The breaking of the contacts points to the perturbation of three-dimensional compactness of cyt *c* and adoption of more labile conformation in the aforementioned fragments of polypeptide chain. Notably, these findings are in excellent harmony with the results of RMSF calculations depicted in Fig. 4. Additional proofs in favor of the above conclusion come from the analysis of cyt *c* spatial structure after the simulation which showed that the width of the heme pocket increases from 0.91 nm in PG40 bilayers up to 1.07 nm in CL25 systems.

CONCLUSIONS

Cumulatively, the molecular dynamics simulation of the examined protein-lipid systems provided evidence for the local destabilization of cyt *c* structure, specific for CL-containing membranes. The analysis of 100 ns trajectories showed that:

- cyt *c* structure does not undergo noticeable perturbations upon its association with either PC/PG or PC/PS lipid bilayers;
- the complexation of cyt *c* with CL-containing membranes is followed by the protein transition into a more labile conformation arising from the widening of the heme crevice and partial unfolding of polypeptide chain mainly in the region Ala15-Leu32;
- increase of CL proportion from 5 to 25 mol% results in the enhancement of fluctuations in the region Pro76-Asp93.

The revealed specific features of cyt *c* – CL interactions may not only be a means of modulating the biological functions of this protein, but may also underlie its transition to the conformations favoring the oligomerization and fibrillization in a membrane-bound state.

ACKNOWLEDGEMENTS

This work was supported by the grant № 0116U000937 for Young Scientists from the Ministry of Science and Education of Ukraine.

REFERENCES

1. Chiti F., Dobson C.M. Protein misfolding, amyloid formation, and human disease: a summary of progress over the last decade // Annu. Rev. Biochem. – 2017. – Vol. 86. – P. 27-68.
2. Kelly J.W. Towards an understanding of amyloidogenesis // Nat. Struct. Biol. – 2002. – Vol. 9. – P. 323-325.
3. Zbilut J. P., Colosimo A., Conti F., Colafranceschi M., Manetti C., Valerio M., Webber Jr. C. L., Giuliani A. Protein aggregation/folding: the role of deterministic singularities of sequence hydrophobicity as determined by nonlinear signal analysis of acylphosphatase and Aβ (1-40) // Biophys. J. – 2003. – Vol. 85. – P. 3544-3557.
4. Seelig J. Thermodynamics of lipid-peptide interactions // Biochim. Biophys. Acta. – 2004. – Vol. 1666. – P. 40-50.
5. Gsponer J., Vendruscolo M. Theoretical approaches to protein aggregation // Protein Pept. Lett. – 2006. – Vol. 13. – P. 287-293.
6. Dill K. A. Dominant forces in protein folding // Biochemistry. – 1990. – Vol. 29. – P. 7133-7155.
7. Bokvist M., Lindstrom F., Watts A., Grobner G. Two types of Alzheimer's β-amyloid (1–40) peptide membrane interactions: aggregation preventing transmembrane anchoring versus accelerated surface fibril formation // J. Mol. Biol. – 2004. – Vol. 335. – P. 1039–1049.
8. Sharp J.S., Forrest J.A., Jones R.A.L. Surface denaturation and amyloid fibril formation of insulin at model lipid-water interfaces // Biochemistry – 2002. – Vol. 41. – P. 15810–15819.
9. Zhao H., Jutila A., Nurminen T., Wickstrom S.A., Keski-Oja J., Kinnunen P.K.J. Binding of endostatin to phosphatidylserine-containing membranes and formation of amyloid-like fibers // Biochemistry. – 2005. – Vol. 44. – P. 2857–2863.
10. Jo E., Darabie A.A., Han K., Tandon A., Frazer P.E., McLaurin J. α-synuclein – synaptosomal membrane interactions. Implications for fibrillogenesis // Eur. J. Biochem. – 2004. – Vol. 271. – P. 3180–3189.
11. Knight J.D., Miranker A.D. Phospholipid catalysis of diabetic amyloid assembly // J. Mol. Biol. – 2004. – Vol. 341. – P. 1175–1187.
12. Chirita C.N., Necula M., Kuret J. Anionic micelles and vesicles induce tau fibrillization *in vitro* // J. Biol. Chem. – 2003. – Vol. 278. – P. 25644–25650.
13. Zhao H., Tuominen E.K.J., Kinnunen P.K.J. Formation of amyloid fibers triggered by phosphatidylserine-containing membranes // Biochemistry. – 2003. – Vol. 43. – P. 10302–10307.
14. Uversky V.N., Fink A.L. Conformational constraints for amyloid fibrillation: the importance of being unfolded // Biochim. Biophys. Acta. – 2004. – Vol. 1698. – P. 131–153.
15. Gorbenko G. P., Kinnunen P. K. J. The role of lipid-protein interactions in amyloid-type protein fibril formation // Chem. Phys. Lipids. – 2006. – Vol. 141. – P. 72-82.
16. Wei G., Mousseau N., Derreumaux P. Computational simulations of early steps of protein aggregation // Prion. – 2007. – Vol. 1. – P. 3-8.
17. Avila C., Drechsel N., Alcantara R., Viila-Freixa J. Multiscale molecular dynamics of protein aggregation // Current Protein and Peptide Science. – 2011. – Vol. 12. – P. 221-234.
18. Beck D., Daggett V. Methods for molecular dynamics simulations of protein folding/unfolding in solution // Methods. – 2004. – Vol. 34. – P. 112-120.

19. Miao Y., Feixas F., Eun C., McCammon J.A. Accelerated molecular dynamics simulations of protein folding // J. Computat. Chem. – 2015. – Vol. 36. – P. 1536-1549.
20. Lemkul J.A., Bevan D.R. Assessing the stability of Alzheimer's amyloid protofibrils using molecular dynamics // J. Phys. Chem. B. – 2010. – Vol. 114. – P. 1652-1660.
21. Diaz-Moreno I., Garcia-Heredia J.M., Diaz-Quitana A., De la Rosa M.A. Cytochrome c signalosome in mitochondria // Eur. Biophys. J. – 2011. – Vol. 40. – P. 1301–1315.
22. Goodsell D.S. The molecular perspective: cytochrome c and apoptosis // The Oncologist. – 2004. – Vol. 9. – P. 226–227.
23. Haldar S., Sil P., Thangamuniyandi M., Chattopadhyay K. Conversion of amyloid fibrils of cytochrome c to mature nanorods through a honeycomb morphology // Langmuir. – 2015. – Vol. 31. – P. 4213–4223.
24. Groot N.S., Ventura S. Amyloid fibril formation by bovine cytochrome c // Spectroscopy. – 2005. – Vol. 19. – P. 199–205.
25. Furkan M., Fazili N.A., Afsar M., Naeem A. Analysing cytochrome c aggregation and fibrillation upon interaction with acetonitrile: an in vitro study // J. Fluoresc. – 2016. – Vol. 26. – P. 1959–1966.
26. Hashimoto M., Takeda A., Hsu L.J., Takenouchi T., Masliah E. Role of cytochrome c as a stimulator of alpha-synuclein aggregation in Lewy body disease // J. Biol. Chem. – 1999. – Vol. 274. – P. 28849−28852.
27. Huang J., MacKerell A. CHARMM36 all-atom additive protein force field: validation based on comparison to NMR data // J. Comput. Chem. – 2013. – Vol. 34. – P. 2135–2145.
28. Lomize M., Pogozheva I., Joo H., Mosberg H., Lomize A. OPM database and PPM web server: resources for positioning of proteins in membranes // Nucl. Acids Res. – 2012. – Vol. 40. – P. 370–376.
29. Jo S., Lim J., Klauda J., Im W. CHARMM-GUI Membrane builder for mixed bilayers and its application to yeast membranes // Biophys. J. – 2009. – Vol. 97. – P. 50–58.
30. Darden T., York D., Pedersen L. Particle mesh Ewald: An N log(N) method for Ewald sums in large systems // J. Chem. Phys. – 1993. – Vol. 98. – P. 10089–10092.
31. Vehlow C., Stehr H., Winkelmann M., Duarte J., Petzold L., Dinse J., Lappe M. CMView: Interactive contact map visualization and analysis // Bioinformatics. – 2011. – Vol. 27. – P. 1573–1574.
32. Cortese J.D., Voglino A.L., Hackenbrock C.R. Multiple conformations of physiological membrane-bound cytochrome c // Biochemistry. – 1998. – Vol. 37. – P. 6402−6409.
33. Lewis R.N.A., McElhaney R.N. The physicochemical properties of cardiolipin bilayers and cardiolipin-containing lipid membranes // Biochim. Biophys. Acta. – 2009. – Vol. 1788. – P. 2069–2079.
34. Rytömaa M., Kinnunen P.K.J. Evidence for two distinct acidic phospholipid-binding sites in cytochrome *c* // J. Biol. Chem. – 1994. – Vol. 269. – P. 1770–1774.
35. Rytömaa M., Mustonen P., Kinnunen P.K.J. Reversible, nonionic, and pH-dependent association of cytochrome c with cardiolipin-phosphatidylcholine liposomes // J. Biol. Chem. – 1992. – Vol. 267. – P. 22243–22248.
36. Kalanhni E., Wallace C.J.A. Cytochrome c impaled: investigation of the extended lipid anchorage of a soluble protein to mitochondrial membrane models // Biochem. J. – 2007. – Vol. 407. – P. 179–187.
37. Sinibaldi F., Howes B.D., Droghetti E., Polticelli F., Piro M.C., Di Pierro D., Fiorucci L., Coletta M., Smulevich G., Santucci R. Role of lysines in cytochrome c–cardiolipin interaction // Biochemistry. – 2013. – Vol. 52. – P. 4578–4588.
38. Hanske J., Toffey J.R., Morenz A.M., Bonilla A.J., Schiavoni K.H., Pletneva E.V. Conformational properties of cardiolipin-bound cytochrome c // Proc. Natl. Acad. Sci. USA. – 2012. – Vol. 109. – P. 125–130.
39. Muenzner J., Pletneva E. Structural transformations of cytochrome c upon interaction with cardiolipin // Chem. Phys. Lipids. – 2014. – Vol. 179. – P. 57–63.
40. Pandiscia L.A., Schweitzer-Stenner R. Coexistence of native-like and non-native partially unfolded ferricytochrome *c* on the surface of cardiolipin-containing liposomes // J. Biol. Chem. B. – 2015. – Vol. 119. – P. 1334–1349.
41. Pinheiro T.J.T., Watts A. Lipid specificity in the interaction of cytochrome c with anionic phospholipid bilayers revealed by solid-state 31P NMR // Biochemistry. – 1994. – Vol. 33. – P. 2451–2458.
42. Pinheiro T.J.T., Cheng H., Seeholzer S.H., Roder H. Direct evidence for the cooperative unfolding of cytochrome c in lipid membranes from H-2H exchange kinetics // J. Mol. Biol. – 2003. – Vol. 303. – P. 617–626.
43. Belikova N.A., Vladimirov Y.A., Osipov A.N., Kapralov A.A., Tyurin V.A., Potapovich M.V., Basova L.V., Peterson J., Kurnikov I.V., Kagan V.E. Peroxidase activity and structural transitions of cytochrome c bound to cardiolipin-containing membranes // Biochemistry. – 2006. – Vol. 45. – P. 4998–5009.
44. Hong Y., Muenzner J., Grimm S.K., Pletneva E.V. Origin of the conformational heterogeneity of cardiolipin-bound cytochrome c // J. Amer. Chem. Soc. – 2012. – Vol. 134. – P. 18713–18723.
45. Brown L., Wuthrich K. NMR and ESR studies of the interactions of cytochrome c with mixed cardiolipin-phosphatidylcholine vesicles // Biochim. Biophys. Acta. – 1977. – Vol. 468. – P. 389–410.
46. De Kruijff B., Cullis P.R. Cytochrome c specifically induces non-bilayer structures in cardiolipin-containing model membranes // Biochim. Biophys. Acta. – 1980. – Vol. 602. – P. 477–490.
47. Bergstrom C.L., Beales P.A., Lv Y., Vanderlick T.K., Groves J.T. Cytochrome c causes pore formation in cardiolipin-containing membranes // Proc. Natl. Acad. Sci. USA. – 2013. – Vol. 110. – P. 6269–6274.
48. Spooner P.J.R., Watts A. Reversible unfolding of cytochrome c upon interaction with cardiolipin bilayers. 2. Evidence from phosphorus-31 NMR measurements // Biochemistry. – 1991. – Vol. 30. – P. 3880–3885.
49. Stepanov G., Gnedenko O., Mol'nar A., Ivanov A., Vladimirov Y., Osipov A. Evaluation of cytochrome c affinity to anionic phospholipids by means of surface plasmon resonance // FEBS Lett. – 2009. – Vol. 583. – P. 97–100.
50. Pinheiro T.J.T. The interaction of horse heart cytochrome c with phospholipid bilayers. Structural and dynamic effects // Biochimie. – 1994. – Vol. 76. – P. 489–500.
51. Hildebrandt P., Heimburg T., Marsh D. Quantitative conformational analysis of cytochrome c bound to phospholipid vesicles studied by resonance Raman spectroscopy // Eur. Biophys. J. – 1990. – Vol. 18. – P. 193–201.
52. Heimburg T., Hildebrandt P., Marsh D. Cytochrome c-lipid interactions studied by resonance Raman and 31P NMR spectroscopy. Correlation between the conformational changes of the protein and lipid bilayer // Biochemistry. – 1991. – Vol.

30. – P. 9084–9089.
53. Muenzner J., Toffey J., Hong Y., Pletneva E. Becoming a peroxidase: cardiolipin-induced unfolding of cytochrome c // J. Phys. Chem. B. – 2013. – Vol. 117. – P. 12878–12886.
54. Mandal A., Hoop C., DeLucia M., Kodali R., Kagan V., Ahn J., Wel P. Structural changes and proapoptotic peroxidase activity of cardiolipin-bound mitochondrial cytochrome c // Biophys. J. – 2015. – Vol. 109. – P. 1873–1884.
55. O'Brien E., Nucci N., Fuglestad B., Tommos C., Wand A.J. Defining the apoptotic trigger the interaction of cytochrome c and cardiolipin // J. Biol. Chem. – 2015. – Vol. 290. – P. 30879–30887.
56. Balakrishnan G., Hu Y., Spiro T. His26 protonation in cytochrome c triggers microsecond β-sheet formation and heme exposure: implications for apoptosis // J. Am. Chem. Soc. – 2012. – Vol. 134. – P. 19061–19069.
57. Bandi S., Bowler B. Probing the dynamics of a His73–heme alkaline transition in a destabilized variant of yeast iso-1-cytochrome c with conformationally gated electron transfer methods // Biochemistry. -2011. – Vol. 50. – P. 10027–10040.